

# Flexible n-i-p thin film silicon solar cells on polyimide foils with textured ZnO:Ga back reflector

[E. Marins<sup>a, b,</sup>](#), [M. Warzecha<sup>a,</sup>](#), [S. Michard<sup>a,</sup>](#), [J. Hotovy<sup>a, c,</sup>](#), [W. Böttler<sup>a,</sup>](#), [P. Alpuim<sup>b,</sup>](#), [F. Finger<sup>a</sup>](#)

<sup>a</sup> Institute of Energy and Climate Research, Photovoltaic (IEK-5), Forschungszentrum Jülich Jülich D-52425, Germany

<sup>b</sup> Department of Physics, University of Minho, Guimarães 4800-058, Portugal

<sup>c</sup> Faculty of Electrical Engineering and Information Technology, Slovak University of Technology, Ilkovicova 3, Bratislava 812 19, Slovakia

## Abstract

In thin film silicon solar cells on opaque substrates in n-i-p deposition sequence where the textured transparent conductive oxide (TCO) layer serves as a back reflector, one can independently optimize the morphology of the TCO layer without compromise on transparency and conductivity of this layer and further adjust the electro-optical properties of the back contact by using additional layers on top of the textured TCO. In the present work, we use this strategy to obtain textured back reflectors for solar cells in n-i-p deposition sequence on non-transparent flexible plastic foils. Gallium doped ZnO (ZnO:Ga) films were deposited on polyimide substrates by DC magnetron sputtering at a temperature of 200 °C. A wet-chemical etching step was performed by dipping the ZnO:Ga covered foil into a diluted HCl solution. The textured ZnO:Ga is then coated with a highly reflective Ag/ZnO double layer. On this back reflector, we develop thin film silicon solar cells with a microcrystalline silicon absorber layer. The current density for the cell with the textured ZnO:Ga layer is  $\sim 23 \text{ mA/cm}^2$ ,  $4 \text{ mA/cm}^2$  higher than the one without such layer, and a maximum efficiency of 7.5% is obtained for a  $1 \text{ cm}^2$  cell.

## Keywords

Microcrystalline silicon; Transparent conducting oxide; Light trapping; Polyimide; Flexible substrate; Solar cells

## 1. Introduction

Flexible thin film silicon solar cells are usually fabricated in the n-i-p deposition sequence in substrate configuration because it allows the use of opaque, light weight substrates, such as plastic sheets or metallic foils [1,2]. The use of such substrates is of interest in thin film silicon solar cell technology because it reduces manufacturing cost by enabling roll-to-roll production [3]. Besides it opens possibilities for applications

36 like better integration into buildings and textiles. The most used substrate materials for  
37 the fabrication of flexible thin film silicon-based solar cells include stainless steel  
38 substrates [4,5], polyimide (PI) [6], polyethylene terephthalate and polyethylene  
39 naphthalate [7,8]. Among the organic polymer substrates, PI has the advantage of a  
40 higher melting point and glass transition temperature, with a smaller thermal shrinkage  
41 [9].

42 For high efficiency of amorphous (a-Si:H) and microcrystalline ( $\mu\text{c-Si:H}$ ) thin film  
43 silicon solar cells, light trapping of the incident light within the silicon absorber layers  
44 becomes crucial in order to further reduce the cell thickness, which leads to reduction of  
45 the light-induced degradation effects for a-Si:H material [10] and higher throughput in  
46 production for both a-Si:H and  $\mu\text{c-Si:H}$  solar cells [2]. Light scattering at the interfaces  
47 is usually achieved by texturing the front transparent conductive oxide (TCO) electrodes  
48 and/or the back reflectors [11–14]. Some TCO materials already have a suitable texture  
49 in the as-deposited state. On plastic foils, ZnO textured in the as-deposited state  
50 obtained by low pressure chemical vapor deposition or 2D periodic structures have been  
51 used to provide light trapping in the active layers of n-i-p devices [2,7]. Sputter-  
52 deposited ZnO can be textured by a post-deposition wet-chemical etching step [15,16].  
53 For the n-i-p deposition sequence in substrate configuration where the textured TCO  
54 serves as a back reflector, this approach has the advantage of using an optimized  
55 morphology of the TCO layer, where the electro-optical properties can be adjusted by  
56 using additional layers on top of the textured TCO. This technique has been used for  
57 solar cells in both p-i-n and n-i-p deposition sequence on transparent glass substrates  
58 [11,17]. In the present work, we use this strategy to obtain textured back reflectors for  
59 n-i-p solar cells on flexible polyimide foil.

60

## 61 2. Experimental details

62 Microcrystalline thin film silicon solar cells were prepared on 10x10 cm<sup>2</sup> and 125  
63 μm thick PI foils. The substrates for smooth cells were covered with a thermally  
64 evaporated 700 nm Ag layer and an 80 nm sputtered ZnO:Ga, both deposited at room  
65 temperature. In order to obtain rough cells, an 800 nm ZnO:Ga layer was deposited  
66 directly on PI by DC magnetron sputtering at a substrate temperature of 200 °C, using a  
67 ZnO:Ga target (99/1 wt.%). The sputtering power density was 100 W. Both, the total  
68 gas pressure of 5x10<sup>-1</sup> Pa as well as the total gas flow rate of 10 sccm were maintained  
69 constant during the deposition process. This layer was textured by a post-deposition  
70 wet-chemical etching in a 0.5% water diluted HCl solution for 30 seconds. The back  
71 contact was finalized with an additional highly reflecting Ag(200 nm)/ZnO(80 nm)  
72 sputtered double layer that conformally covers the textured ZnO:Ga surface.

73 The thin film silicon layers were deposited in n-i-p sequence by plasma enhanced  
74 chemical vapor deposition using very high frequency excitation (81.36 MHz). The  
75 substrate temperature was 200 °C for intrinsic and doped layers. The power density and  
76 chamber pressure for deposition of intrinsic layers were 210 mW/cm<sup>2</sup> and 100 Pa,  
77 respectively. Doped layers were deposited at power densities and pressures of 470  
78 mW/cm<sup>2</sup> and 300 Pa for n-layers, and 140 mW/cm<sup>2</sup> and 100 Pa for p-layers. The silane  
79 concentration ratio, defined as [SiH<sub>4</sub>] / ([SiH<sub>4</sub>]+[H<sub>2</sub>]), was varied between 5% and 7%  
80 for intrinsic layers.

81 The front transparent contacts made of 70 nm thick indium tin oxide (ITO) layers  
82 were prepared by radio-frequency (RF) magnetron sputtering at room temperature using  
83 a In<sub>2</sub>O<sub>3</sub>:SnO<sub>2</sub> target (95/5 wt.%) in an argon/oxygen atmosphere with relative oxygen  
84 content, defined as [O<sub>2</sub>] / [O<sub>2</sub>+Ar], of 0.1%.

85 The individual solar cells with an area of  $1 \times 1 \text{ cm}^2$  were defined by using a shadow  
86 mask during ITO deposition on the  $10 \times 10 \text{ cm}^2$  substrate. Front metal finger electrodes  
87 were prepared by silver evaporation. Finally, standard annealing procedure of finished  
88 solar cells was performed in air at  $160^\circ\text{C}$  for 30 minutes. The complete device layer  
89 sequences were for smooth cells: PI/Ag/TCO/n-i-p/ITO and for rough cells: PI/textured  
90 ZnO:Ga/Ag/TCO/n-i-p/ITO. Fig. 1 shows schematics of the solar cells on PI on smooth  
91 (Fig. 1.a) and rough (Fig. 1.b) back reflectors.

92 For comparison solar cells were also deposited on glass substrates with the same  
93 layer sequences.

94 The solar cell parameters open circuit voltage ( $V_{oc}$ ), fill factor (FF) and short circuit  
95 current density ( $J_{sc}$ ) were determined from current-voltage (I-V) measurements under  
96 simulated AM1.5G illumination at  $25^\circ\text{C}$ . The external quantum efficiency (EQE) was  
97 obtained from spectral response measurements in the range of 300-1100 nm. The  
98 integrated current from the EQE curves under short circuit conditions was used to  
99 calculate the conversion efficiency in order to avoid possible effects from current  
100 collection around the  $1 \text{ cm}^2$  solar cells or from imprecision in determination of the cell  
101 area.

102 Raman spectroscopy was used to evaluate the crystalline volume fraction of the  
103 intrinsic layers in the solar cells. Raman measurements were performed directly on the  
104 solar cells using a Nd:YAG laser with excitation wavelength of 532 nm.

105

### 106 3. Results and discussion

107 Fig. 2 shows the performance parameters of solar cells deposited on the smooth  
108 PI/Ag(700 nm)/ZnO(80 nm) substrate as a function of silane concentration (SC) of the  
109 *i*-layer. For reference and in order to assess the effect of the substrate on the

110 performance of the solar cells, we prepared identical cells on smooth glass covered with  
111 a standard Ag/ZnO back reflector, optimized for glass substrate. We observed a similar  
112 trend of the performance parameters for the cells on PI when compared to the ones on  
113 glass. However, the  $V_{oc}$  was around 20-40 mV lower for the cells on PI. A reason for the  
114 lower  $V_{oc}$  could be the higher *i*-layer crystallinity of the cells deposited on PI as  
115 measured by Raman spectroscopy on the solar cells. This is shown in fig. 3. Why the PI  
116 substrate possibly promotes the growth of films with higher crystalline volume fraction  
117 is not clear at the moment. Despite of the apparent higher crystallinity in the *i*-layer of  
118 the solar cells prepared on PI with respect to the ones prepared on glass, the  $J_{sc}$  is lower  
119 for cells deposited at SC below 6% where one would instead expect higher absorption at  
120 higher crystallinity. We speculate that this results from absorption losses in the Ag/ZnO  
121 back contact [11], due to the higher roughness of the PI substrate compared to the glass  
122 one. The cell deposited with SC of 6.1% showed the highest  $V_{oc}$  (505 mV) and FF of  
123 70.7%. For this reason we chose the deposition conditions of this cell for further  
124 optimization of the solar cells on PI with rough TCO. Fig. 4 shows the I-V curve of this  
125 solar cell on smooth PI and on glass substrate with an *i*-layer thickness of 1.8  $\mu\text{m}$   
126 deposited at SC = 6.1%, which yields a current density of 18.9  $\text{mA}/\text{cm}^2$  on PI and 20.7  
127  $\text{mA}/\text{cm}^2$  on glass.

128 To further enhance the current of cells on PI, we developed ZnO:Ga layers for  
129 application as textured back reflector [18]. This development was first carried out on  
130 glass and later transferred to application on the PI substrate.

131 Fig. 5 shows the EQE of a solar cell prepared on ZnO:Ga deposited on PI, textured  
132 by post-deposition wet-chemical etching in HCl solution for 30 seconds, and covered  
133 with a highly reflecting Ag/ZnO double layer. For comparison the EQE of the cell on  
134 flat PI is shown. We observe a strong increase in EQE especially above 600 nm for the

135 cell with the textured ZnO:Ga layer accompanied by efficient reduction of interference  
136 fringes. The cell on structured TCO delivers a current density of  $\sim 23 \text{ mA/cm}^2$ , more  
137 than  $4 \text{ mA/cm}^2$  higher than the one on flat PI, and an efficiency of 7.5% is achieved for  
138 a  $1 \text{ cm}^2$  cell. However, the FF decreased from 70.7% to 68%, and the  $V_{oc}$  was 30 mV  
139 lower. These reductions in FF and  $V_{oc}$  are expected and related to the roughness of the  
140 substrate [19]. The improvement in current was observed essentially for wavelengths  
141 above 650 nm, corresponding to the light trapping region for microcrystalline solar cells  
142 [11]. Fig. 6 shows the corresponding IV curve of this cell and, for comparison, the curve  
143 of an identical cell deposited on a standard textured TCO/Ag/ZnO back reflector on  
144 glass.

145 Results presented above and summarized in table 1 showed that the well-  
146 established technology of post-deposition textured TCO films as a scattering layer to  
147 promote light trapping in thin film silicon solar cells can be transferred to application  
148 with flexible plastic substrates.

149

150

#### 151 4. Conclusions

152 We have presented our development of microcrystalline single-junction n-i-p thin  
153 film silicon solar cells on flexible polyimide substrate. The results of solar cells on  
154 smooth PI showed similar behavior in terms of performance parameters in comparison  
155 to cells deposited on smooth glass. The  $V_{oc}$  was around 20-40 mV lower for the cells on  
156 PI, which is related to higher *i*-layer crystallinity of cells on PI. We developed a  
157 textured ZnO:Ga layer to promote light trapping in the solar cells on PI that yield more  
158 than  $23 \text{ mA/cm}^2$  on absorbers of  $1.8 \mu\text{m}$  thickness with cell efficiencies of up to 7.5%.

159

160 **Acknowledgements**

161       One of the authors (E. Marins) thanks FCT (Fundação para a Ciência e Tecnologia)  
162 for the PhD grant SFRH/BD/46740/2008. We would like to acknowledge A. Schmalen,  
163 J. Wolff, M. Hülsbeck and W. Reetz for the technical support, and A. Doumit, J. Worbs  
164 and H. Siekmann for the depositions of the front and back contacts. The first author  
165 thanks Dr. Ü. Dagkaldiran for the important advices and discussions during this work.

166

167 **References**

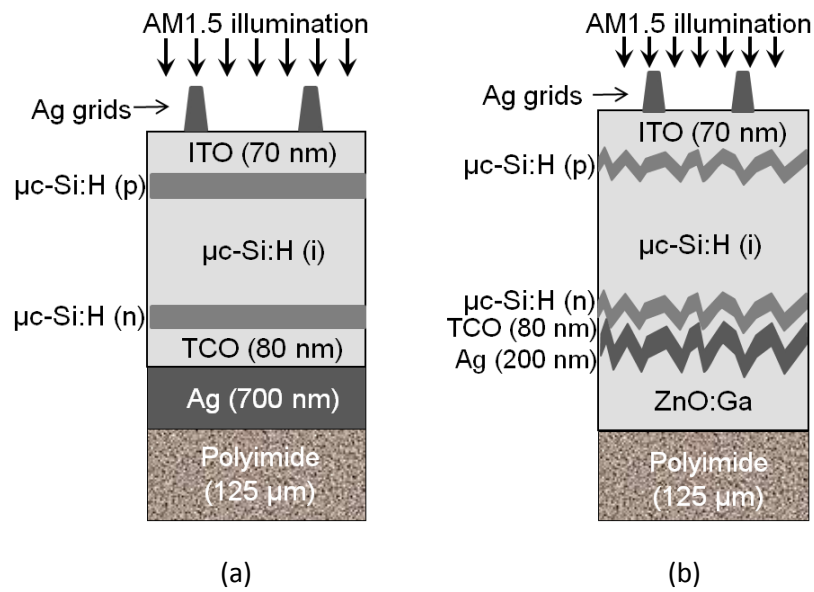
- 168 [1] A. Banerjee, S. Guha, Study of back reflectors for amorphous silicon alloy solar cell  
169 application, *J. Appl. Phys.* 69 (1991) 1030–1035.
- 170 [2] T. Söderström, F.-J. Haug, X. Niquille, C. Ballif, TCOs for nip thin film silicon solar  
171 cells, *Prog. Photovoltaics Res. Appl.* 17 (2009) 165–176.
- 172 [3] J. Bailat, V. Terrazzoni-Daudrix, J. Guillet, F. Freitas, X. Niquille, A. Shah, C. Ballif, T.  
173 Scharf, R. Morf, A. Hansen, D. Fischer, Y. Ziegler, A. Closset, Recent development of  
174 solar cells on low-cost plastic substrates, in: *Proc. 20th Eur. PVSEC*, 2005: pp. 1529–  
175 1532.
- 176 [4] J. Yang, A. Banerjee, S. Guha, Triple-junction amorphous silicon alloy solar cell with  
177 14.6 % initial and 13.0 % stable conversion efficiencies, *Appl. Phys. Lett.* 70 (1997)  
178 2975–2977.
- 179 [5] K. Saito, M. Sano, H. Otsoshi, A. Sakai, S. Okabe, K. Ogawa, High efficiency large area  
180 solar cells using microcrystalline silicon, in: *Proc. 3rd World PVSEC*, Osaka, 2003: pp.  
181 2793–2798.
- 182 [6] M. Tanda, K. Tabuchi, M. Uno, S. Kato, Y. Takeda, S. Iwasaki, Y. Yokohama, T. Wada,  
183 M. Shimosawa, Y. Sakakibara, A. Takano, H. Nishihara, H. Enomoto, T. Kamoshita,  
184 Large area, light weight, flexible solar cell production technology-ready for the market  
185 entry, in: *Proc. 31st IEEE PVSC*, IEEE, Lake Buena Vista, 2005: pp. 1560–1563.
- 186 [7] F.-J. Haug, T. Söderström, M. Python, V. Terrazzoni-Daudrix, X. Niquille, C. Ballif,  
187 Development of micromorph tandem solar cells on flexible low-cost plastic substrates,  
188 *Sol. Energy Mater. Sol. Cells.* 93 (2009) 884–887.
- 189 [8] P. Alpuim, G.M. Junior, S.A. Filonovich, P. Roca i Cabarrocas, J.-E. Bouree, E.V.  
190 Johnson, Y.M. Soro, Polymorphous and nanocrystalline silicon thin-film solar cells  
191 deposited at 150°C on plastic substrates, in: *Proc. 23rd Eur. PVSEC*, 2008: pp. 2455–  
192 2458.
- 193 [9] K. Tao, D. Zhang, L. Wang, J. Zhao, H. Cai, Y. Sui, Z. Qiao, Q. He, Y. Zhang, Y. Sun,  
194 Development of textured back reflector for n–i–p flexible silicon thin film solar cells,  
195 *Sol. Energy Mater. Sol. Cells.* 94 (2010) 709–714.
- 196 [10] D.L. Staebler, C.R. Wronski, Reversible conductivity changes in discharge produced  
197 amorphous Si, *Appl. Phys. Lett.* 31 (1977) 292–294.
- 198 [11] J. Müller, B. Rech, J. Springer, M. Vanecek, TCO and light trapping in silicon thin film  
199 solar cells, *Sol. Energy.* 77 (2004) 917–930.
- 200 [12] S. Fay, L. Feitknecht, R. Schlüchter, U. Kroll, E. Vallat-Sauvain, A. Shah, Rough ZnO  
201 layers by LP-CVD process and their effect in improving performances of amorphous and  
202 microcrystalline silicon solar cells, *Sol. Energy Mater. Sol. Cells.* 90 (2006) 2960–2967.
- 203 [13] J. Hüpkas, B. Rech, O. Kluth, T. Repmann, B. Zwaygardt, J. Müller, R. Drese, M.  
204 Wuttig, Surface textured MF-sputtered ZnO films for microcrystalline silicon-based  
205 thin-film solar cells, *Sol. Energy Mater. Sol. Cells.* 90 (2006) 3054–3060.



- 206 [14] T. Tohsophon, J. Hüpkes, H. Siekmann, B. Rech, M. Schultheis, N. Sirikulrat, High rate  
207 direct current magnetron sputtered and texture-etched zinc oxide films for silicon thin  
208 film solar cells, *Thin Solid Films*. 516 (2008) 4628–4632.
- 209 [15] O. Kluth, B. Rech, L. Houben, S. Wieder, G. Schöpe, C. Beneking, H. Wagner, A. Löffl,  
210 H.W. Schock, Texture etched ZnO:Al coated glass substrates for silicon based thin film  
211 solar cells, *Thin Solid Films*. 351 (1999) 247–253.
- 212 [16] W. Böttler, V. Smirnov, J. Hüpkes, F. Finger, Variation of back reflector morphology in  
213 n-i-p microcrystalline silicon thin film solar cells using texture-etched ZnO, *J. Non.*  
214 *Cryst. Solids*. (2012) 2474–2477.
- 215 [17] W. Böttler, V. Smirnov, A. Lambertz, J. Hüpkes, F. Finger, Window layer development  
216 for microcrystalline silicon solar cells in n-i-p configuration, *Phys. Status Solidi C*. 7  
217 (2010) 1069–1072.
- 218 [18] M. Warzecha, PhD Thesis, Forschungszentrum Jülich, 2012.
- 219 [19] T. Söderström, F.-J. Haug, V. Terrazzoni-Daudrix, C. Ballif, Optimization of amorphous  
220 silicon thin film solar cells for flexible photovoltaics, *J. Appl. Phys.* 103 (2008) 114509–  
221 1–114509–8.
- 222
- 223

224 **List of figure and table captions**

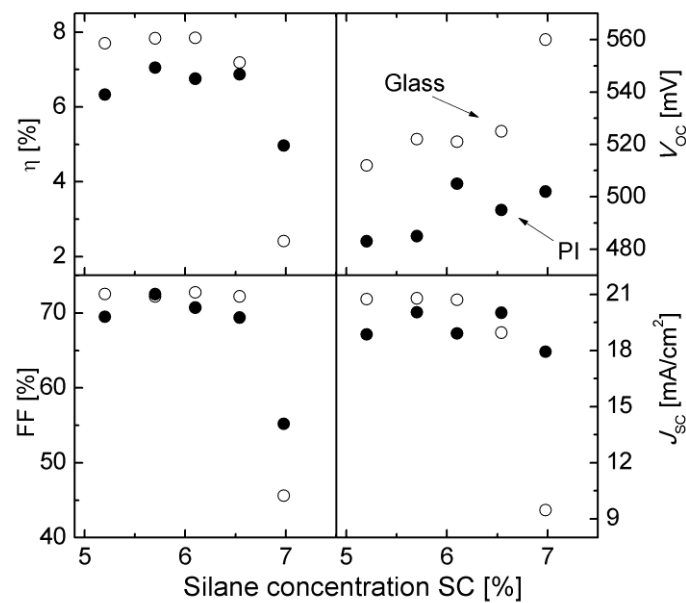
225



226

227 **Fig. 1:** Structures of the solar cells on PI without (a) and with (b) textured ZnO:Ga  
 228 layer.

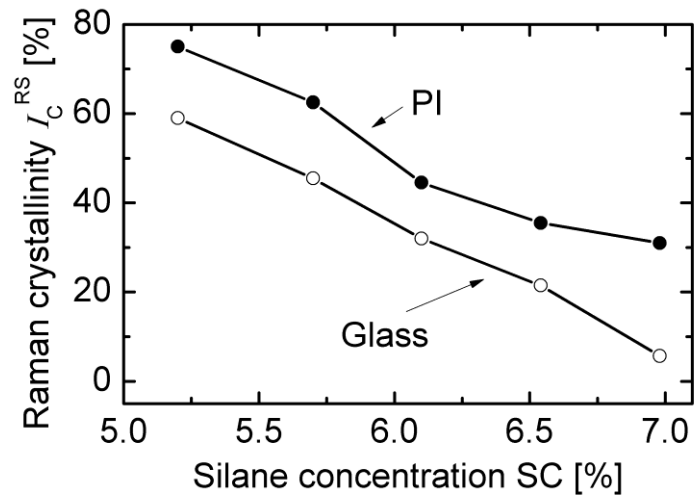
229



230

231 **Fig. 2:** I-V parameters of solar cells with different *i*-layer silane concentrations  
 232 deposited on PI/Ag/ZnO (full symbols) and glass/Ag/ZnO (open symbols).

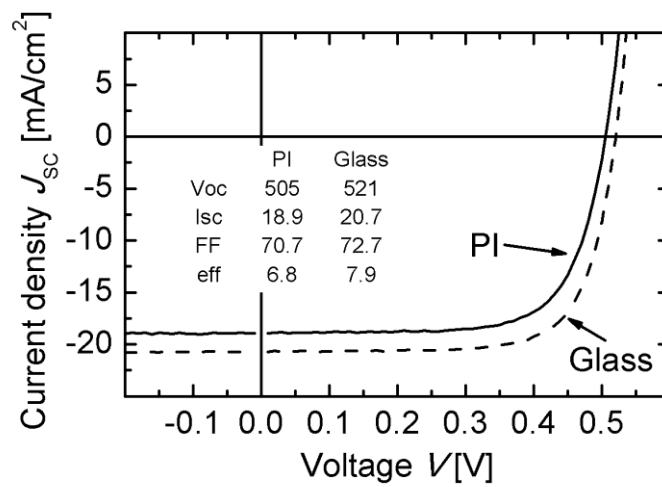
233



234

235 **Fig. 3:** Raman crystallinity as a function of the *i*-layer silane concentration of solar cells  
 236 deposited on PI (full symbols) and glass (open symbols). Lines are guides to the eye.

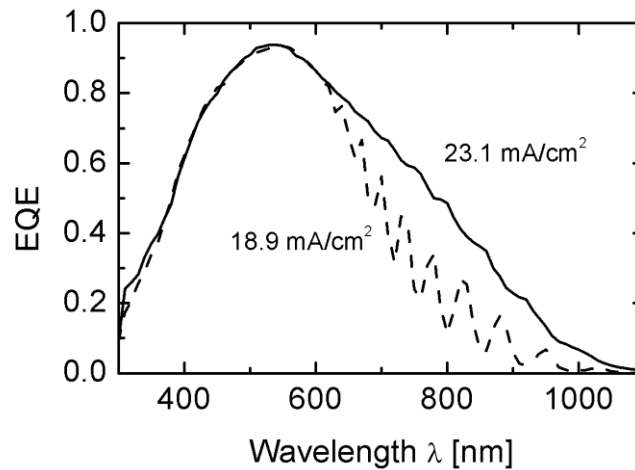
237



238

239 **Fig. 4:** Comparison of the I-V curves of solar cells on PI/Ag/ZnO (plain curve) and  
 240 glass/Ag/ZnO (dashed curve).

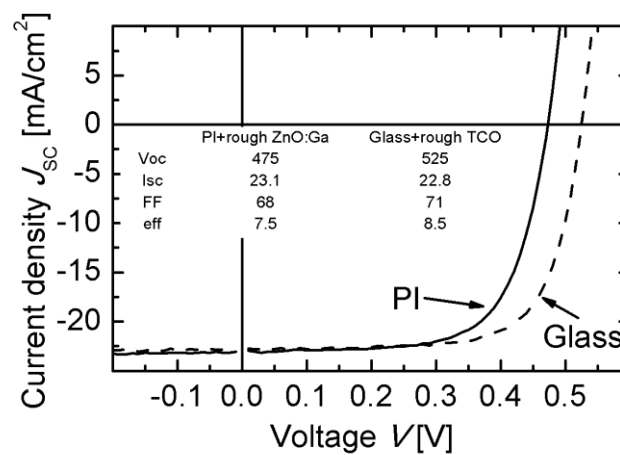
241



242

243 **Fig. 5:** Comparison of EQE's of solar cells on PI/Ag/ZnO (dashed line) and PI/textured  
244 ZnO:Ga/Ag/ZnO (full line).

245



246

247 **Fig. 6:** Comparison of the I-V curves of solar cells on PI/textured ZnO:Ga /Ag/ZnO  
248 (plain curve) and glass/textured TCO/Ag/ZnO (dashed curve).

249

250 **Table 1:** I-V parameters of solar cells under AM1.5 illumination.

Substrate type	Voc (mV)	J <sub>sc</sub> (mA/cm <sup>2</sup> )	FF (%)	η (%)
Smooth glass	521	20.7	72.7	7.9
Smooth PI	505	18.9	70.7	6.8
Glass+rough TCO	525	22.8	71	8.5
PI+rough ZnO:Ga	475	23.1	68	7.5

251